STM JOURNALS

Journal of
Industrial Safety Engineering

ISSN: 2395-6674
Volume 11, Issue 1, 2024
January–Aprill
DOI (Journal): 10.37591/JoISE

https://journals.stmjournals.com/joise/

Research JoISE

Behavior of R.C. Buildings with Steel Encased Elements Subjected to Impact Loads

Shaikh Md. Junaid[1,*], R.S. Londhe[2]

Abstract

This study examines the resilience of steel-encased concrete column beams and frames against blast loads, a crucial concern in regions prone to terrorist threats or accidental explosions. An exhaustive literature review establishes the historical context and theoretical frameworks of blast-resistant design. The research employs finite element analysis (FEA) simulations to study the dynamic behavior of these structures under various blast scenarios, revealing insights into load distribution, deformation, and failure mechanisms. By integrating blast-resistant design principles, numerical simulations, and innovative mitigation strategies, the dissertation advances structural engineering practices for blast-resistant construction. The findings offer practical solutions to enhance the resilience of steel-encased concrete structures, providing valuable guidance for engineers, researchers, and policymakers dedicated to protecting the built environment from blast threats.

Keywords: Blast analysis, Dynamic performance, Steel encased concrete columns.

INTRODUCTION

The Steel Reinforced Concrete (SRC), also known as steel in concrete shell, is widely utilized for its superior load-bearing capacity, high strength, and excellent seismic resistance. The bond between steel and concrete in SRC structures provides remarkable structural integrity, making them ideal for earthquake-prone areas and enhancing fire resistance due to the concrete cover. However, SRC construction faces challenges such as spatial collisions between longitudinal reinforcement and section steel. Common solutions, like cutting bars and welding, increase costs and complexity. Another issue is closing stirrups due to spatial collisions, often requiring drilling holes in section walls or flanges, adding further complexity [1–5].

Moreover, the proximity of rebar and sections can deteriorate concrete quality, especially in members with high proportions of sections or rebar. This necessitates placing reinforcing cages outside the steel form, increasing concrete cover thickness but potentially compromising bending capacity and shear strength.

***Author for Correspondence**
Shaikh Md. Junaid
E-mail: sshaikh_gca@rediffmail.com

[1]P.G. Student, Department of Applied Mechanics, Government Engineering College, Aurangabad, Maharashtra, India
[2]Associate Professor & Head, Department of Applied Mechanics, Government Engineering College, Aurangabad, Maharashtra, India

Received Date: June 15, 2024
Accepted Date: June 27, 2024
Published Date: June 28, 2024

Citation: Shaikh Md. Junaid, R.S. Londhe. Behaviour of R.C. Buildings with Steel Encased Elements Subjected to Impact Loads. Journal of Industrial Safety Engineering. 2024; 11(1): 20–36p.

To address these challenges, Steel Fiber Reinforced Concrete (SFRC) has emerged as a viable solution. SFRC inhibits crack propagation and enhances tensile strength, shear strength, and energy dissipation. Building on SFRC, a novel approach is proposed: Steel and Steel Fiber Reinforced Concrete (SSFRC) structures. SSFRC replaces traditional reinforcement with steel fibers, aiming to enhance flexural capacity, shear strength, and material bonding while simplifying construction and reducing costs [6–9].

SSFRC structures eliminate labour-intensive processes such as cutting and welding, streamlining

construction and reducing costs. They allow closer placement of steel flanges to cross-section edges, optimizing structural elements and improving performance and efficiency. SSFRC structures maintain SRC's advantages while avoiding construction difficulties, improving concrete quality by providing ample space for pouring. Steel fibres can replace stirrups and shear pins, enhancing usability and durability without stiffening frames. Thus, SSFRC structures offer improved structural performance, simplified construction, and reduced costs, presenting a promising solution for future construction projects [10–12].

Some previous literatures have suggested that such structural elements may prove to be efficient in resisting quassi-static and impact forces to a considerable extent. This Study was intended in analysing the behaviour of such composite elements so as to resist blast or other impact loads which may be subjected to a structural element due to various phenomena.

SIGNIFICANCE OF ASSESSMENT

Assessing explosion risks in structural design is challenging due to the unpredictability of potential hazards, ranging from accidental to intentional explosions. The primary goal of load assessment is to establish an acceptable threat threshold, which, when exceeded, prompts the implementation of protective measures such as structural reinforcements, blast-resistant materials, or strategic building layouts. Despite these efforts, no building can be completely immune to all threats, which can evolve due to changes in technology, tactics, or geopolitical factors. Thus, structural designers must adopt flexible strategies that allow for adjustments to meet evolving safety requirements.

Designing structures to withstand explosions also necessitates considering nearby buildings, which can amplify an explosion's impact and pose additional challenges. Various explosive sources, including military weapons, improvised explosive devices (IEDs), and industrial accidents, must be considered. Blast loads exhibit unique characteristics such as rapid pressure changes, shock waves, and high-velocity debris, requiring specialized design considerations to ensure structural integrity and occupant safety.

Incorporating explosion mitigation strategies during the initial design stages is crucial. Nonlinear design approaches help absorb and dissipate explosion energy, enhancing building resilience. Figure 1illustrates the pressure changes over time during a free-air blast wave. Initially, pressure matches the ambient level (Po). Upon the shock front's arrival (tA), pressure spikes to peak overpressure (Pso) almost instantaneously. As the shock wave travels outward, both peak overpressure and velocity diminish. Pressure gradually returns to ambient levels during the positive phase (to), followed by a negative phase with pressures below ambient, causing suction forces that can eject glass fragments outward. Although lower than during the positive phase, these pressures are significant when assessing a building's overall performance under blast loading.

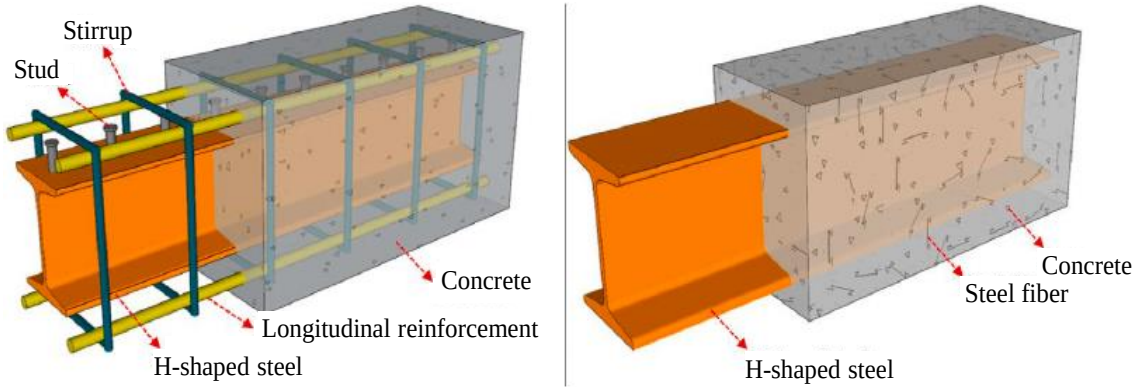

Figure 1. Extruded View of (a) SRC (b) SSFRC.

To accurately design structures to withstand blast loads, equations suggested by researchers like Friedlander and standards such as IS-4991 provide valuable tools for calculating pressure values and understanding blast wave dynamics. These equations enable engineers to develop resilient structures capable of withstanding the complex forces generated by explosive events.

$$P_s = P_{So}\left(1 - \frac{t}{t_0}\right)e - \alpha\frac{t}{t_0} \tag{1}$$

The decay Pressure Q0, can be calculated by the suggested equation of IS-4991 which is stated below.

$$Q = Q_0\left(1 - \frac{t}{t_0}\right)^2 e - 2\alpha\frac{t}{t_0} \tag{2}$$

For relatively thinner components that are flexible, however, the negative phase should also be modelled. It can be noted from Figure 2 that blast loading is associated with very high magnitude and frequency; hence it needs special attention

PRECURSORY LITERATURES

To identify the contributions in this research area and uncover potential research gaps, previous literature on composite structures and impact loading simulations was studied and analysed. The following sections review and elaborate on these key studies:

Kai Wu, et al. [1] investigated composite beam elements to reduce reinforcement build-up, proposing steel-steel fiber reinforced concrete (SSFRC) structures. Eighteen SSFRC beams with varying cross-sectional ratios, steel fiber volumes, and shear span ratios underwent four-point bending tests. The study analyzed failure modes, load-deflection curves, and energy dissipation-based ductility coefficients, finding that increased steel fiber volume and profiled steel ratios significantly enhance strain capacity, ductility modulus, and energy dissipation. A failure mechanism combining bending and shear forces at the joint between steel sections and steel fiber reinforced concrete was proposed fig 2-3.

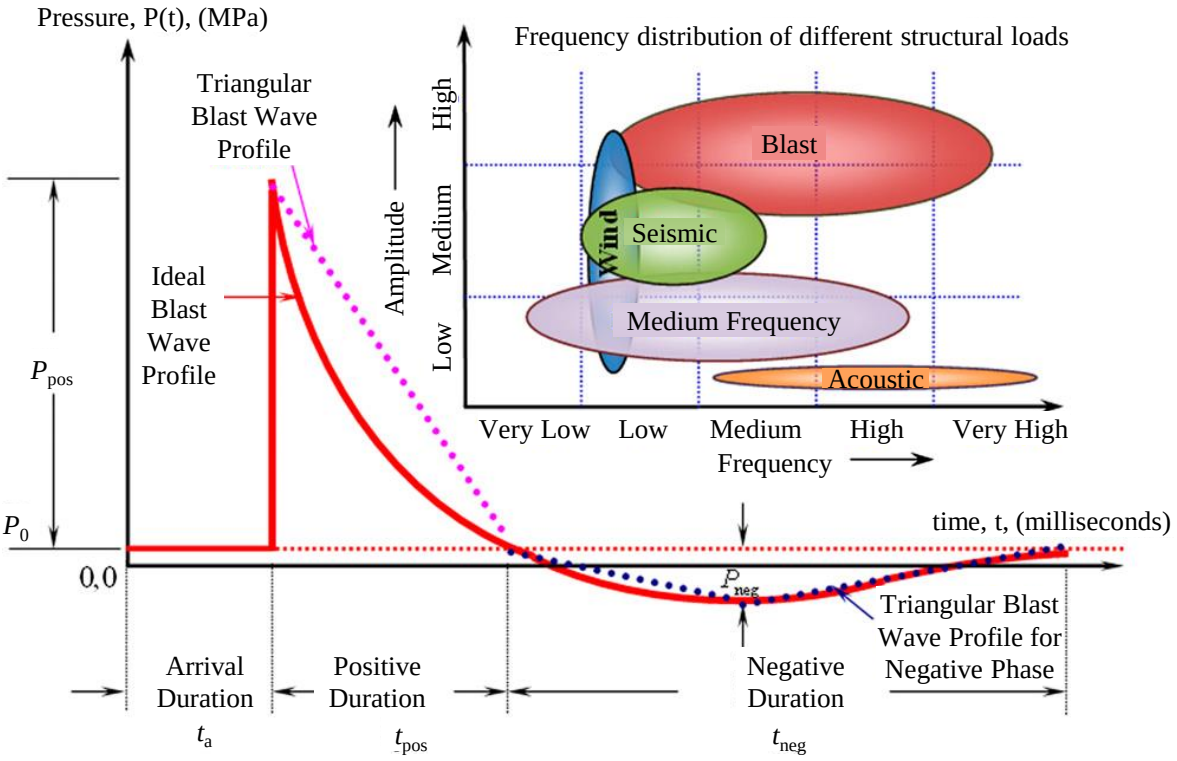

Figure 2. Representation of actual and idealised wave.

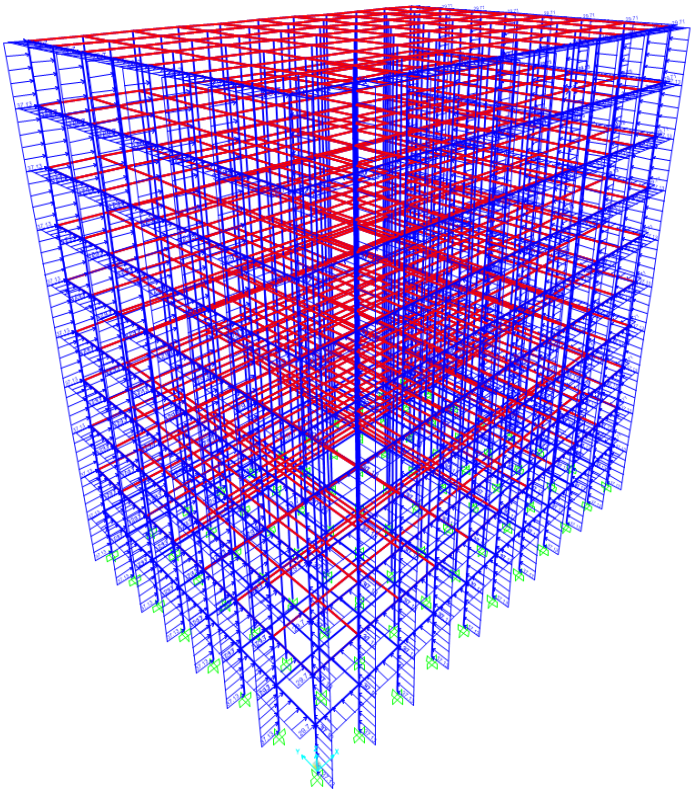

Figure 3. Illustration of a typical bare frame model subjected to Blast loads.

Ji-Hun Choi, et al. [2] evaluated the blast resistance of prestressed concrete elements through numerical and experimental assessments of bi-directional unbounded prestressed concrete surfaces. Using CONWEP program simulations, the study found PSC and PSRC specimens to have higher rigidity and shear strength than RC specimens, with fewer macrocracks. Increased concrete compressive strength improved blast resistance, and PSRC samples outperformed RC and PSC samples under ultimate load conditions.

Zubair I. Syed, et al. [3] examined earthquake-resistant framed reinforced concrete structures' performance during explosions, using IBC 2009 and ACI 318-11 standards. A 14-story precast concrete structure was analyzed under varying explosion distances (4 to 16 m) and TNT weights (50, 100, 200, 500 kg) using ETABS 2013 software. The study aimed to determine safe distances for earthquake-resistant structures and assessed the impact of explosion location.

Manmohan Dass Goel and Vasant Matsagar [4] researched blast-resistant design, focusing on material responses, mitigation techniques, and sacrificial blast walls. They emphasized increasing standoff distances, optimizing mass distribution, and utilizing lighter, energy-absorbing materials like advanced metal foam to reduce peak reflective overpressure.

Mohammed Alias Yusof, et al. [5] modeled reinforced concrete blast walls subjected to impact loading with AUTODYN 3D hydro-coding software, analyzing charge weights from 5 kg to 1500 kg TNT. The study found walls withstand charges up to 50 kg TNT but fail with 400 kg TNT or more. AUTODYN simulations accurately assessed structural threats without physical testing.

Yasser E. Ibrahim, et al. [6] investigated reinforced concrete frame buildings' response to blast loads using ABAQUS for finite element analysis. A four-story building model with different reinforcement scenarios was tested with a 1-tonne TNT charge. Results showed significant damage to columns directly exposed to blast pressures, with confined steel tube columns performing better than standard designs.

B.M. Luccioni, et al. [7] analyzed building collapse under blast loads using Hydrocode. Simulating 400 kg TNT explosions at various heights, they validated numerical models with actual damaged structures, showing complete damage to columns and beams. The study highlighted the importance of correlating real explosion damage with numerical simulations for effective post-blast structural analysis[8-12].

METHODOLOGY

Based on the literature reviewed and the research gaps identified, the following approach has been established for this work. A total of 16 model simulations were conducted using analytical tools capable of simulating and analyzing detonations. The models and their descriptions are detailed Table 1 below:

Table 1. System Development

S.N.	Model Designation	Model	Description
1.	ECB-100A	Steel encased concrete beam structures with 100 kg TNT with 20 m Standoff distance	These structures consist only beams which are reinforced using rolled sections, all other sections will be of conventional concrete. This structure has been analyzed for 100 kg TNT
2.	ECB-100B	Steel encased concrete beam structures with 100 kg TNT with 30 m Standoff distance	These structures consist only beams which are reinforced using rolled sections, all other sections will be of conventional concrete. This structure has been analyzed for 100 kg TNT
3.	ECB-200A	Steel encased concrete beam structures with 200 kg TNT with 20 m Standoff distance	These structures consist only beams which are reinforced using rolled sections, all other sections will be of conventional concrete. This structure has been analyzed for 200 kg TNT
4.	ECB-200B	Steel encased concrete beam structures with 200 kg TNT with 30 m Standoff distance	These structures consist only beams which are reinforced using rolled sections, all other sections will be of conventional concrete. This structure has been analyzed for 200 kg TNT
5.	ECC-100A	Steel encased concrete column structures with 100 kg TNT with 20 m Standoff distance	These structures consist only columns which are reinforced using rolled sections, all other sections are of conventional concrete. These structures have been analyzed for 100 kg TNT at 20 m Standoff distance
6.	ECC-100B	Steel encased concrete column structures with 100 kg TNT with 30 m Standoff distance	These structures consist only columns which are reinforced using rolled sections, all other sections are of conventional concrete. These structures have been analyzed for 100 kg TNT at 30 m Standoff distance
7.	ECC-200A	Steel encased concrete column structures with 200 kg TNT with 20 m Standoff distance	These structures consist only columns which are reinforced using rolled sections, all other sections are of conventional concrete. These structures have been analyzed for 200 kg TNT at 20 m Standoff distance
8.	ECC-200B	Steel encased concrete column structures with 200 kg TNT with 30 m Standoff distance	These structures consist only columns which are reinforced using rolled sections, all other sections are of conventional concrete. These structures have been analyzed for 200 kg TNT at 30 m Standoff distance
9.	ECS-100A	Steel encased concrete structures with 100 kg TNT with 20 m Standoff distance	Column and beam sections in these structures are reinforced using rolled sections. These structures have been analyzed for 100 kg TNT at 20 m Standoff distance
10.	ECS-100B	Steel encased concrete structures with 100 kg TNT with 30 m Standoff distance	Column and beam sections in these structures are reinforced using rolled sections. These structures have been analyzed for 100 kg TNT at 30 m Standoff distance
11.	ECS-200A	Steel encased concrete structures with 200 kg TNT with 20 m Standoff distance	Column and beam sections in these structures are reinforced using rolled sections. These structures have been analyzed for 200 kg TNT at 20 m Standoff distance
12.	ECS-200B	Steel encased concrete structures with 200 kg TNT with 30 m Standoff distance	Column and beam sections in these structures are reinforced using rolled sections. These structures have been analyzed for 200 kg TNT at 30 m Standoff distance
13.	CCS-100A	Conventional concrete structures with 100 kg TNT with 20 m Standoff distance	These Structure were Conventional Concrete Structures and have been analyzed for 100 kg TNT at 20 m Standoff distance

14.	CCS-100B	Conventional concrete structures with 100 kg TNT with 30 m Standoff distance	These Structure were Conventional Concrete Structures and have been analyzed for 100 kg TNT at 30 m Standoff distance
15.	CCS-200A	Conventional concrete structures with 200 kg TNT with 20 m Standoff distance	These Structure were Conventional Concrete Structures and have been analyzed for 200 kg TNT at 20 m Standoff distance
16.	CCS-200B	Conventional concrete structures with 200 kg TNT with 30 m Standoff distance	These Structure were Conventional Concrete Structures and have been analyzed for 200 kg TNT at 30 m Standoff distance

On the basis of the developed system 16 models are analysed for different cases.

a. Conventional concrete frames were analyzed for different magnitude of blasts with different stand-off distances.
b. Composite frames were analyzed for different magnitude of blasts with different stand-off distances.
c. Blast was simulated using triangular time history function.
d. Blast loads were applied on the structure in the form of UDL worked out from the peak pressure values fig 4 -11 and table 3-4.

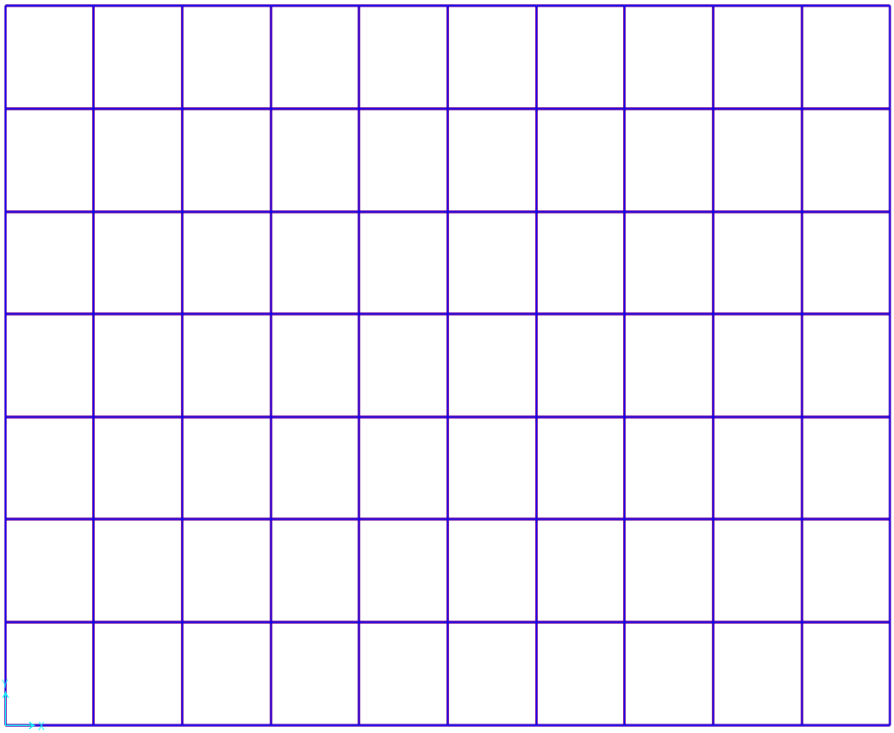

Figure 4. Illustration of a typical bare frame model subjected to Blast loads.

Table 2. Geometrical Properties

1.	**Plan Type**	**Rectangular Shaped**
2.	Plan Dimensions	(30 × 21) m
3.	No. of bays along X/Y	10/7
4.	Width of each bay	3.0 m
5.	Height of the structure	30 m
6.	Height of each storey	3.0 m
7.	Thickness of Slabs	150 mm
8.	Internal / External Wall thickness	150 mm
9.	Depth of footings	3.0 m

Table 3. Loading Data

1.	Grade of concrete	M35
2.	Grade of reinforcing steel	Fe-500
3.	Density of concrete	25 KN/m^3
4.	Density of brick masonry	19 KN/m^3
5.	Column Section	750 × 750 mm
6.	Beam Section	300 × 600 mm
7.	Slab Thickness	150 mm
8.	Explosion Magnitudes	100/200 kg TNT
9.	Standoff distances	20/30 m
10.	Method of Analysis	Triangular Non-Linear Time History Analysis
11.	Calculation of Impact forces	IS-4991 (1968)

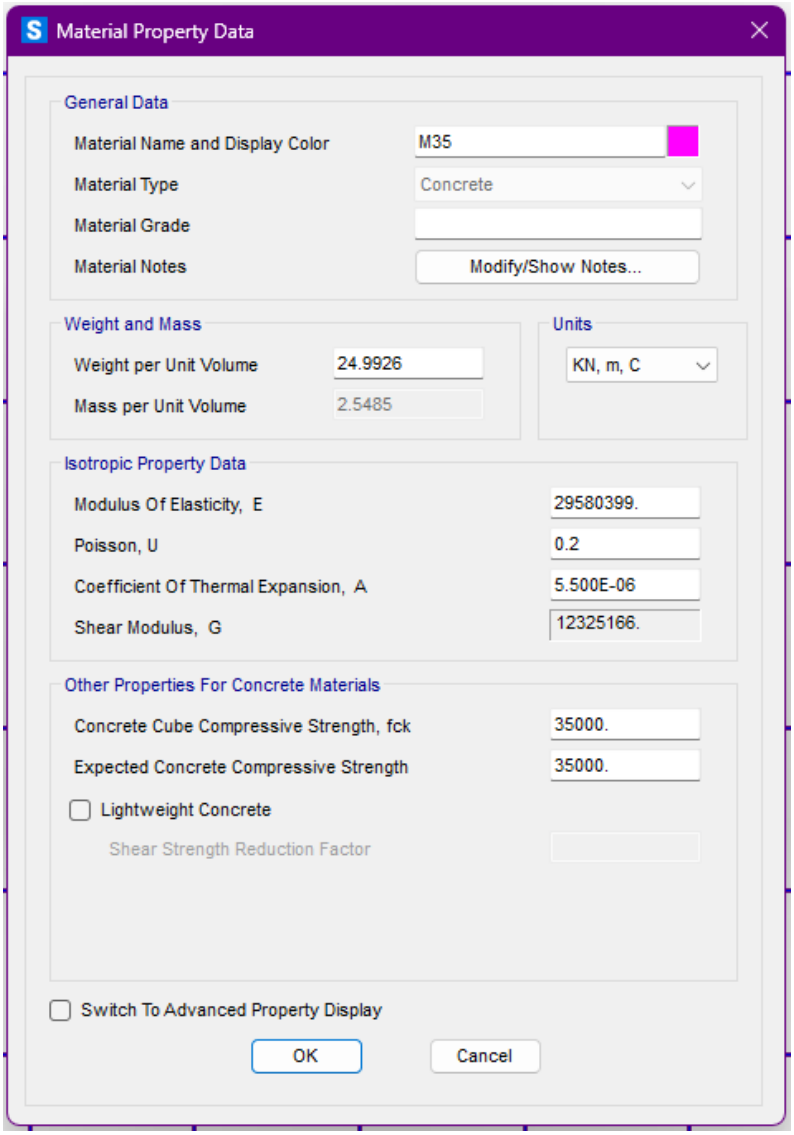

Figure 5. Material Property- (Concrete).

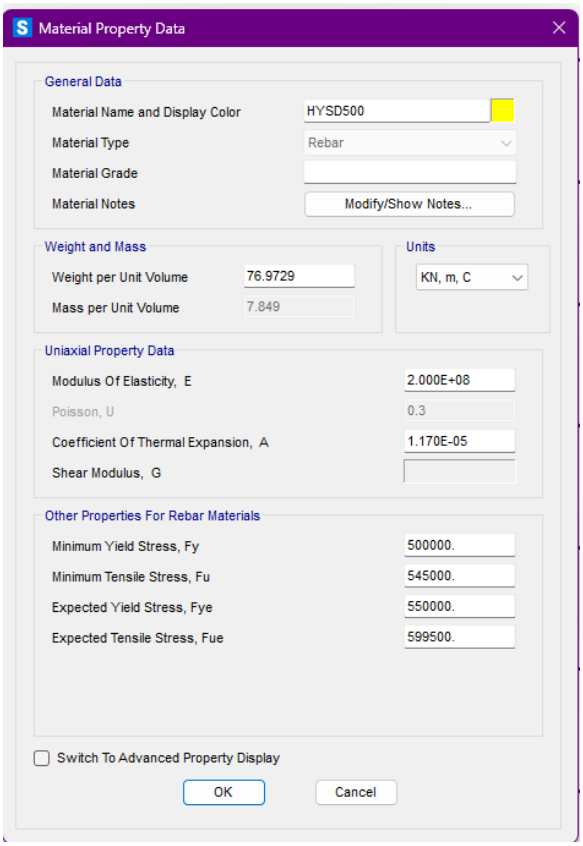

Figure 6. Material Property- (Rebar).

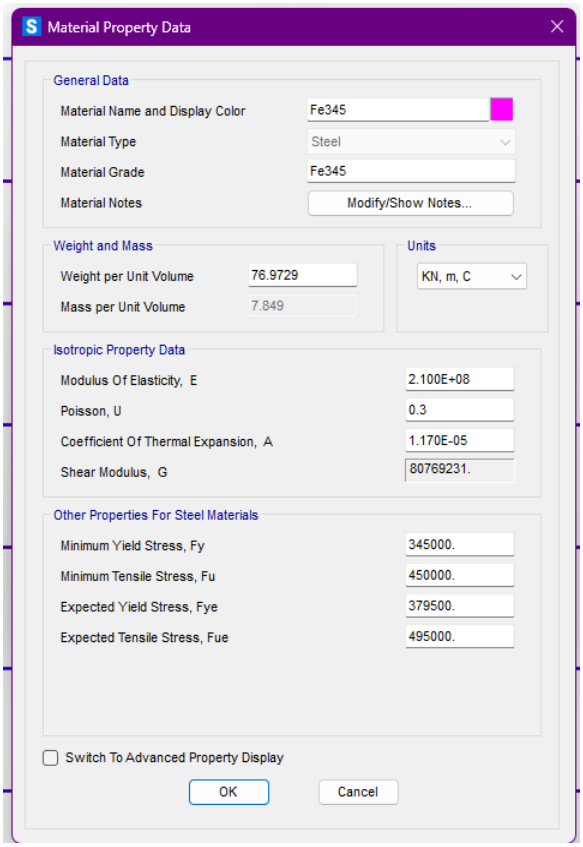

Figure 7. Material Property- (Steel).

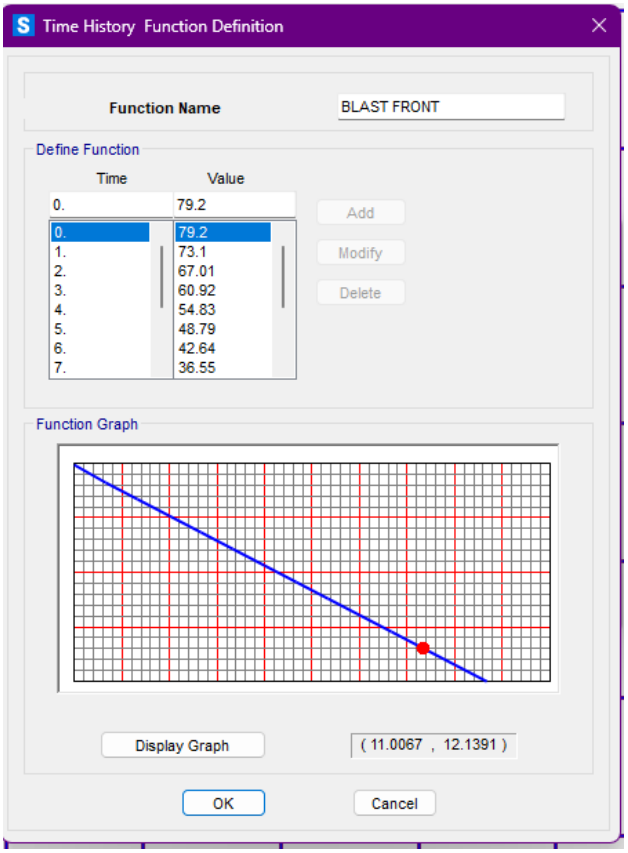

Figure 8. Time History Analysis (Blast Front Triangular History).

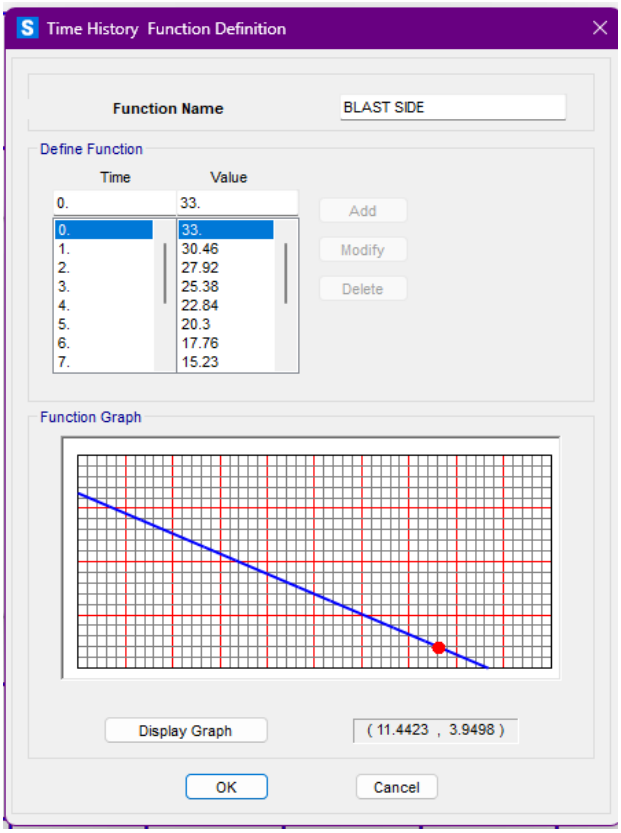

Figure 9. Time History Analysis (Blast Side- Triangular History).

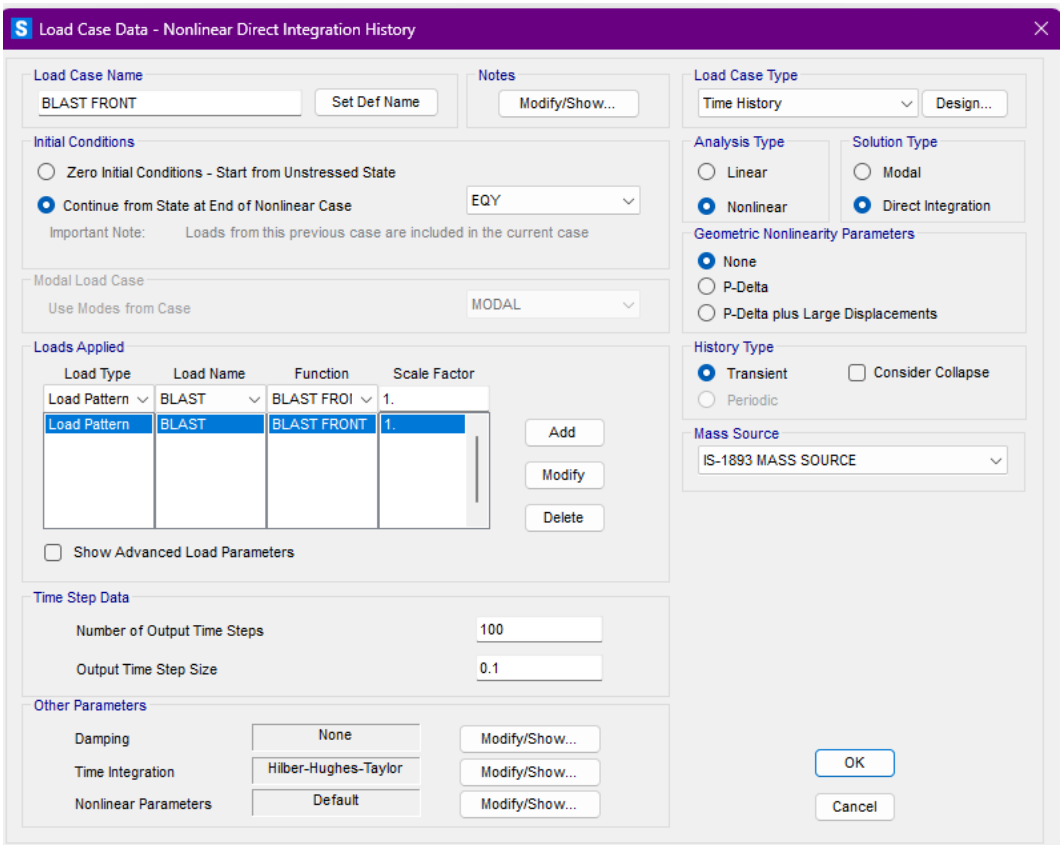

Figure 10. Time History Load Cases (Blast Front).

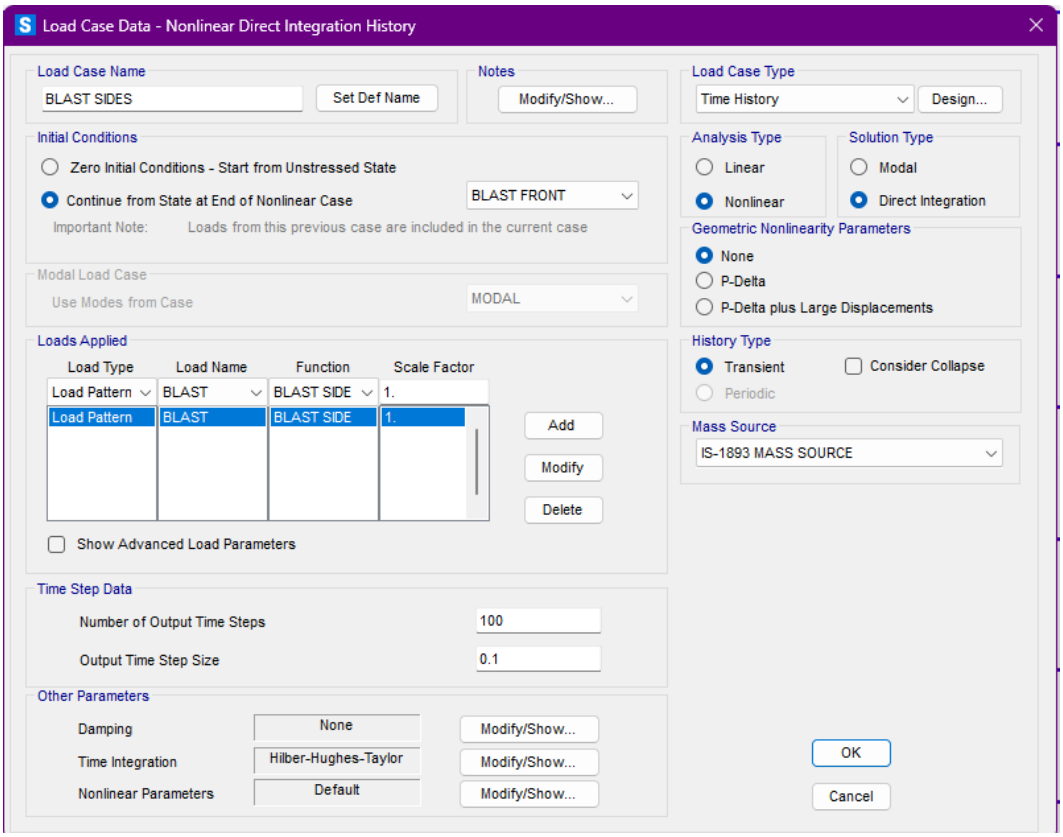

Figure 11. Time History Load Cases (Blast Side).

PERFORMANCE ANALYSIS

Impact load calculations (Blast, IS-4991)

The load calculation as described in the previous heads basically depends upon the magnitude of detonation which was 100 and 200 kg for this study, hence the typical calculations for 100 kg TNT has been specified below:

Impact Load Calculations for 100 kg TNT

For 100 kg TNT at 30 m stand-off distance, the various parameters have been considered as below:

a. Scaled Distance (X) = 64.63 m
b. Peak Side Overpressure (P_{so}) = 0.353 kg/cm^2
c. Mach No. (M) = 1.144
d. Positive Phase Duration (T_0) = 17.52 Mil. Sec.
e. Equivalent Triangular Pulse Duration (T_d) = 13.16 Mil. Sec.
f. Dynamic Pressure ratio T_0/T_d = 0.041
g. Peak Reflected Overpressure Ratio = 0.792

Maximum Displacements for 100 and 200 kg TNT

The maximum displacement is the most significant parameter while assessing the impacts & dynamic loads on the structures. The maximum displacement of different structures has been shown in the Table 4-7 Figure 12-15.

Table 4. Maximum Displacements -ECB Models.

Story	ECB-200B (mm)	ECB-200A (mm)	ECB-100B (mm)	ECB-100A (mm)
Story 10	34.56	108.01	13.21	19.69
Story 9	32.88	102.74	12.27	18.28
Story 8	32.03	100.11	11.79	17.57
Story 7	31.19	97.47	11.32	16.87
Story 6	30.35	94.84	10.85	16.16
Story 5	29.50	92.20	10.37	15.46
Story 4	28.66	89.56	9.90	14.75
Story 3	27.82	86.93	9.43	14.04
Story 2	26.97	84.29	8.95	13.34
Story 1	26.13	81.66	8.48	12.63
Base	25.06	78.31	5.17	7.71

Table 5. Maximum Displacements -ECC Models.

Story	ECC-200B (mm)	ECC-200A (mm)	ECC-100B (mm)	ECC-100A (mm)
Story 10	20.2986	63.4311	4.1877	6.2451
Story 9	19.7316	61.6491	6.3828	9.5013
Story 8	18.873	58.968	6.2451	9.3069
Story 7	18.0873	56.5218	5.6214	8.3754
Story 6	17.4474	54.513	5.6214	8.3754
Story 5	17.0343	53.2251	5.2326	7.7922
Story 4	17.6499	55.161	4.8276	7.1847
Story 3	17.5041	54.6912	4.6494	6.9336
Story 2	14.5476	45.4653	5.0463	7.5168
Story 1	20.2986	63.4311	4.1877	6.2451
Base	19.7316	61.6491	6.3828	9.5013

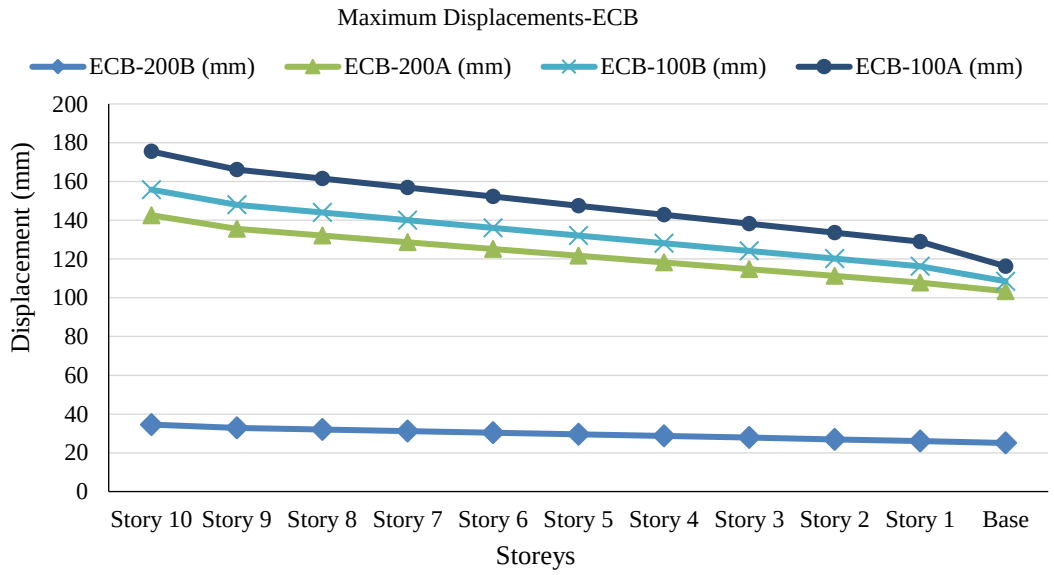

Figure 12. Maximum Displacements-ECB Models.

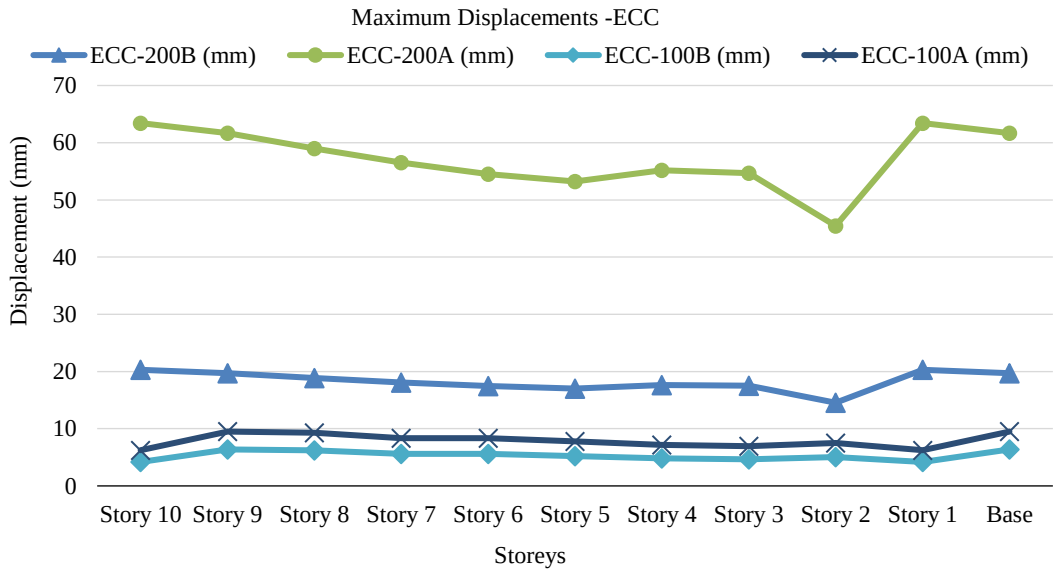

Figure 13. Maximum Displacements-ECC Models.

Table 6. Maximum Displacements-ECS Models.

Story	ECS-200B (mm)	ECS-200A (mm)	ECS-100B (mm)	ECS-100A (mm)
Story 10	14.41	45.04	2.97	4.43
Story 9	14.01	43.77	4.53	6.75
Story 8	13.40	41.87	4.43	6.61
Story 7	12.84	40.13	3.99	5.95
Story 6	12.39	38.70	3.99	5.95
Story 5	12.09	37.79	3.72	5.53
Story 4	12.53	39.16	3.43	5.10
Story 3	12.43	38.83	3.30	4.92
Story 2	10.33	32.28	3.58	5.34
Story 1	14.41	45.04	2.97	4.43
Base	14.01	43.77	4.53	6.75

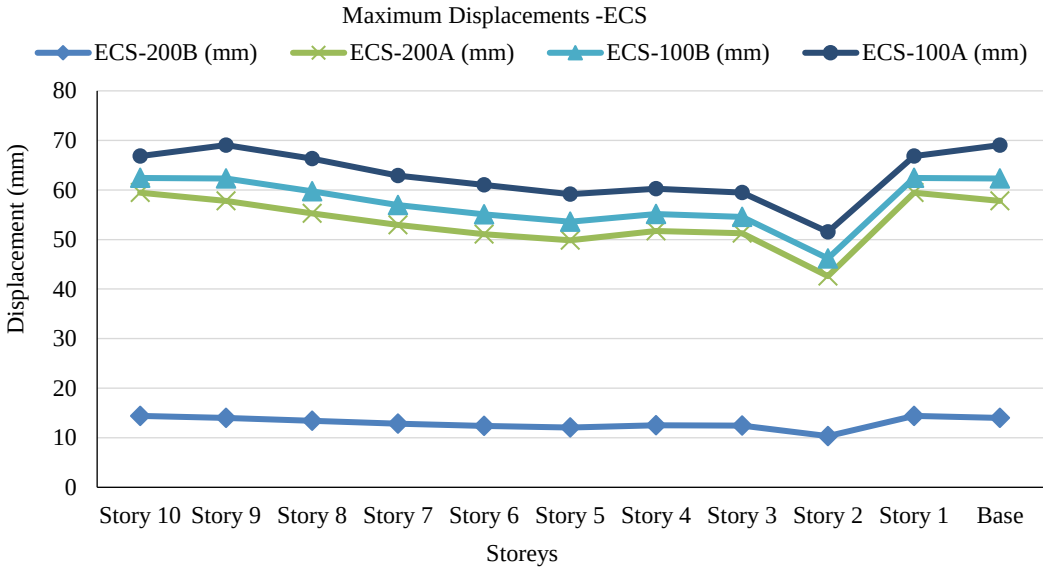

Figure 14. Maximum Displacements-ECS Models.

Table 7. Maximum Displacements-CCS Models.

Story	CCS-200B (mm)	CCS-200A (mm)	CCS-100B (mm)	CCS-100A (mm)
Story 10	51.84	162.02	19.82	29.54
Story 9	49.32	154.11	18.41	27.42
Story 8	48.05	150.17	17.69	26.36
Story 7	46.79	146.21	16.98	25.31
Story 6	45.53	142.26	16.28	24.24
Story 5	44.25	138.30	15.56	23.19
Story 4	42.99	134.34	14.85	22.13
Story 3	41.73	130.40	14.15	21.06
Story 2	40.46	126.44	13.43	20.01
Story 1	39.20	122.49	12.72	18.95
Base	37.59	117.47	7.76	11.57

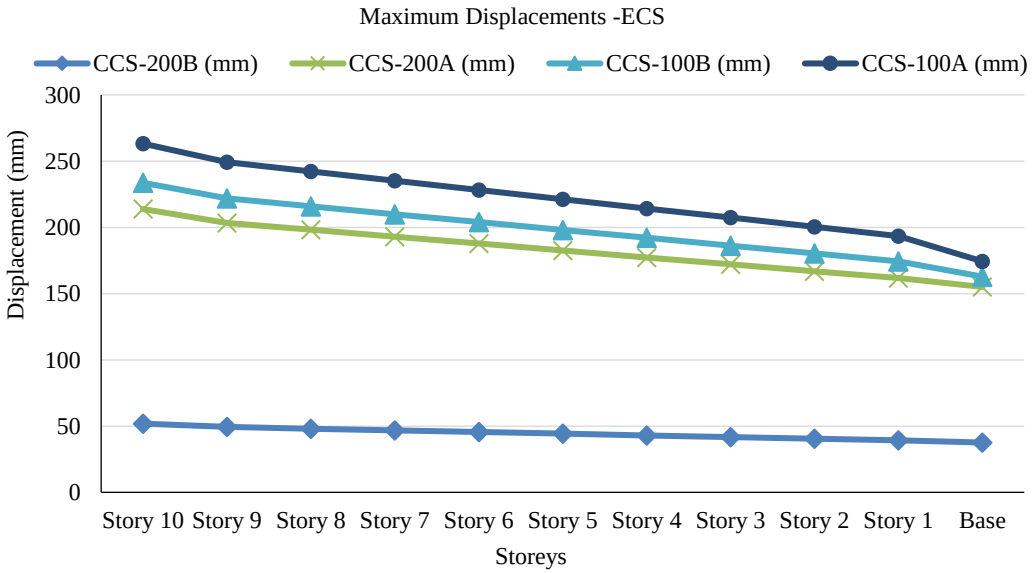

Figure 15. Maximum Displacements-CCS Models.

Acceleration Functions

After the displacements were checked, the next result was checked for the story accelerations. The figures shown below indicates results for the acceleration of various Figure 16-19:

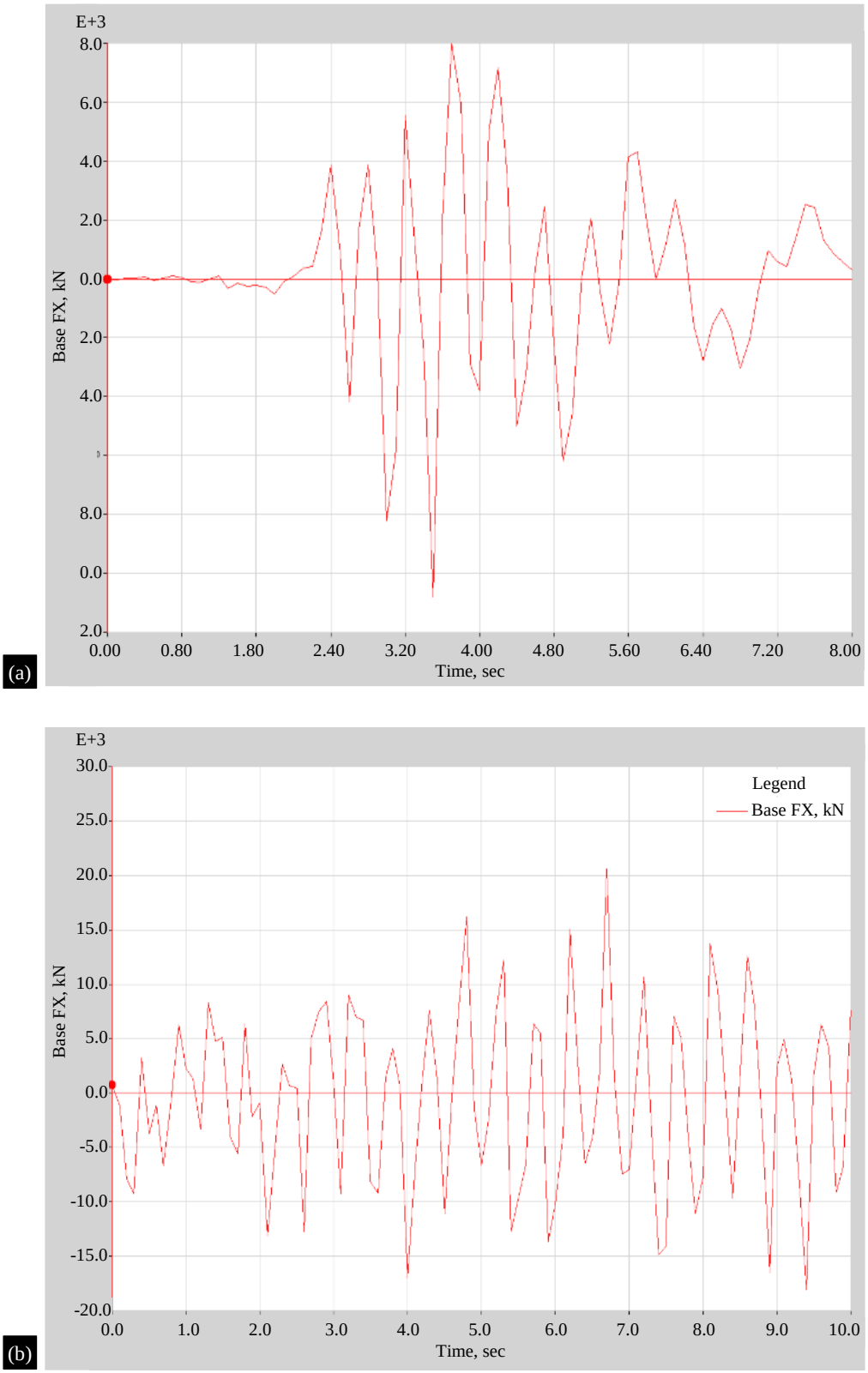

Figure 16. Acceleration function for ECS Frames.

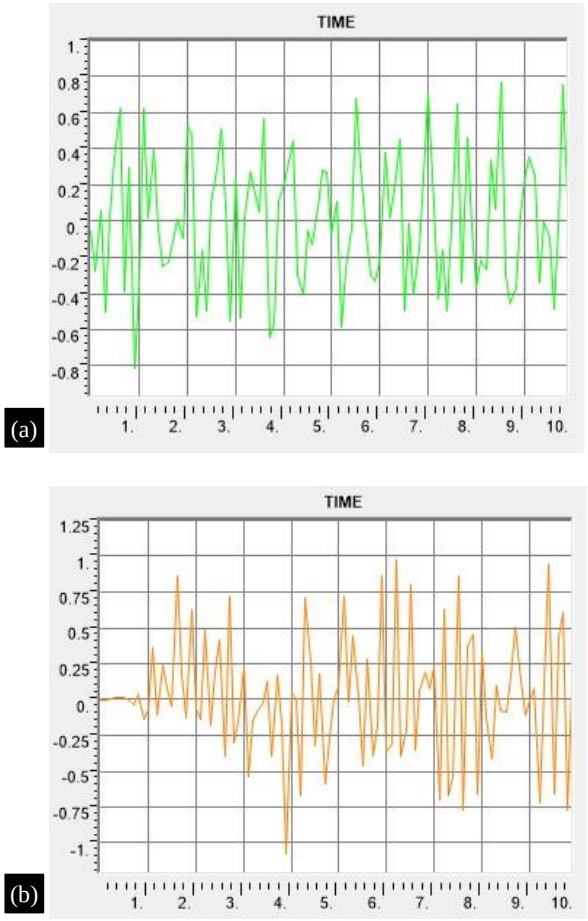

Figure 17. Acceleration function for ECB Frames.

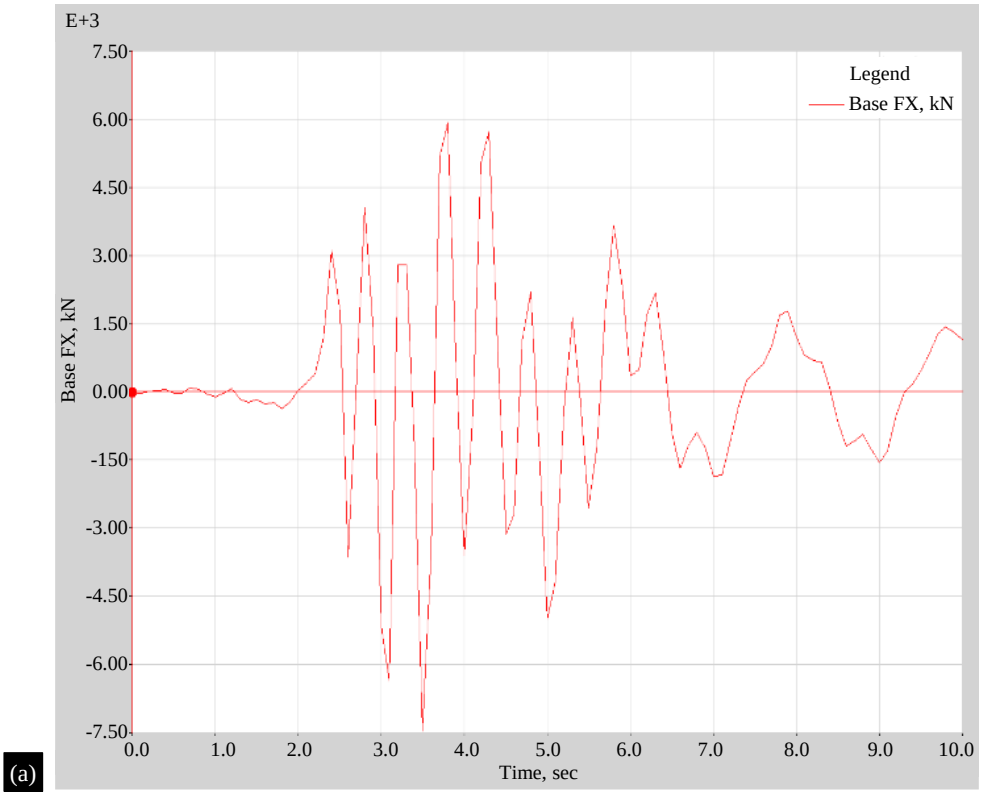

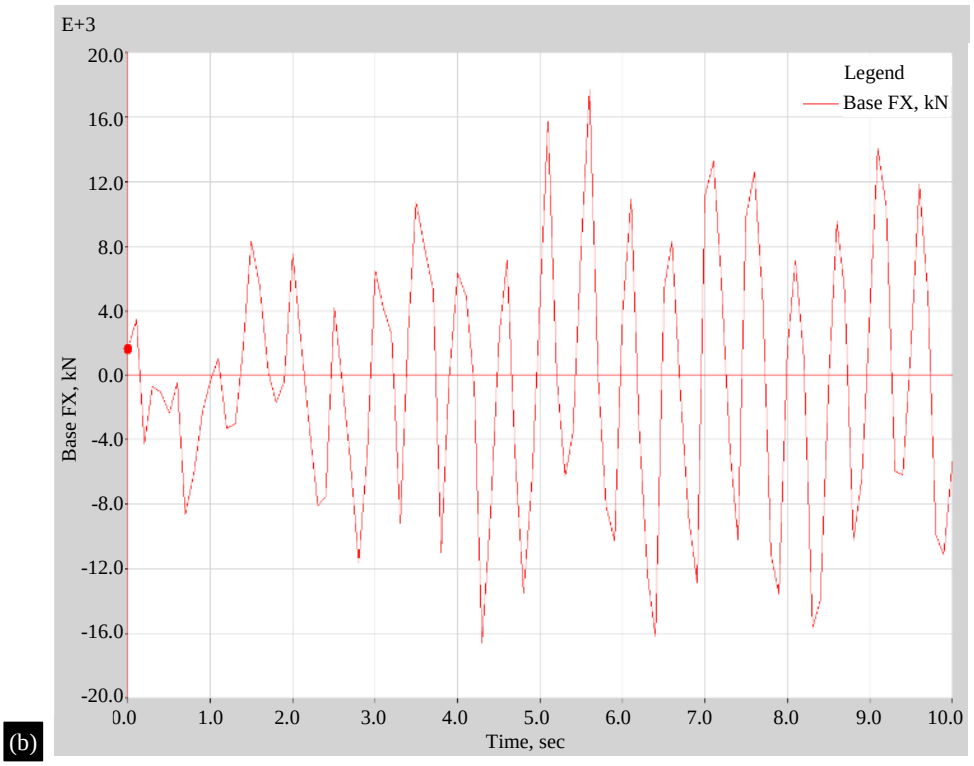

Figure 18. Acceleration function for ECS Frames.

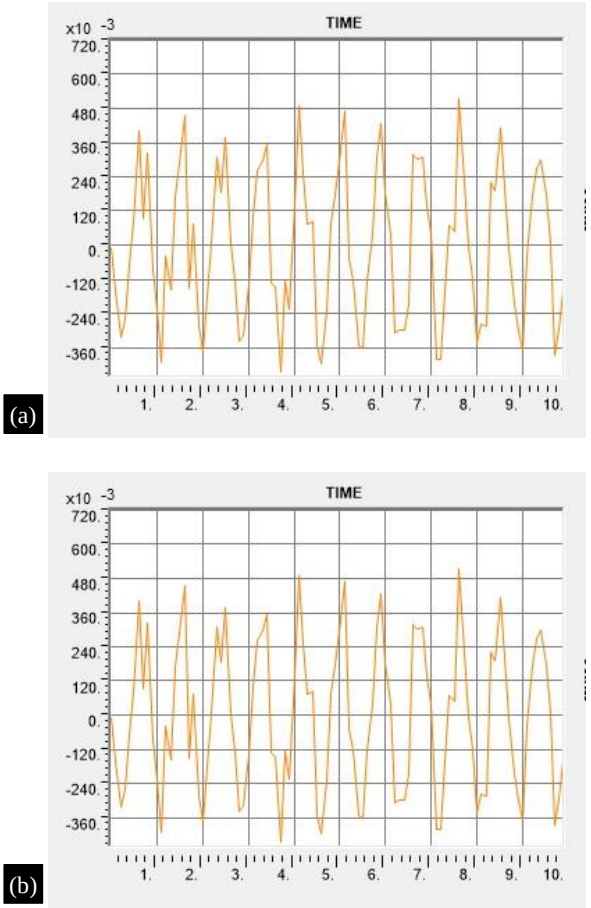

Figure 19. Acceleration function for CCS Frames.

CONCLUSIONS

1. The analytical results indicate that ECB-100 models show approximately a 43% reduction in displacements compared to ECB-200 models.
2. The maximum displacements further decrease by about 63% when comparing ECB to ECC models. This suggests that columns with encased steel elements are more effective in mitigating the adverse effects of blasts under impact loading than encased beams.
3. In the third case, where both encased beams and encased columns (ECS) are used, the structure demonstrates a 79% improvement in resistance to displacements compared to other models.
4. The acceleration functions also follow a similar pattern to the displacement comparisons.
5. Therefore, it is recommended to use concrete-encased columns and concrete-encased frames in structures vulnerable to blast loads, as they reduce the risk of failure by 50-70% compared to conventional concrete structures.

REFERENCES

1. Kai Wu, Feng Chen, Junfu Lin, Jixiang Zhao, Huiming Zheng, "Experimental study on the interfacial bond strength and energy dissipation capacity of steel and steel fibre reinforced concrete (SSFRC) structures", Engineering Structures, Elsevier, Volume 235, 2021, 112094, PP. 17-31.
2. Ji Hun Choi, "Evaluation of blast resistance and failure behaviour of prestressed concrete under blast loading", Construction and Building Materials, Elsevier, 173 (2018) PP. 550–572.
3. Zubair I. Syed, Osama A. Mohamed, Kumail Murad, Manish Kewalramani, "Performance of Earthquake-Resistant RCC Frame Structures under Blast Explosions." International High Performance Built Environment Conference (2016), PP. 82-90
4. Manmohan Das Goel, M. D., Matsagar, V. A., Gupta, A. K., and Marburg, S. (2012). "An abridged review of blast wave parameters." Def. Sci. Journal., Volume 62(5), PP. 300–306.
5. Yusof M.A, Nor NM, Yahya MA, Munikan V, Ismail A. "Prediction of Air Blast Pressure for Military and Commercial Explosive Using Ansys Autodyn", Defence S&T Technical Bulletin. Volume 12(2), May 2019, PP. 77-93
6. Ibrahim, Yasser E., and Marwa Nabil. "Assessment of structural response of an existing structure under blast load using finite element analysis." Alexandria Engineering Journal, Volume 58.4, (2019), PP1327-1338.
7. Luccioni, Bibiana Maria, Ricardo Daniel Ambrosini, and Rodolfo Francisco Danesi. "Analysis of building collapse under blast loads." Engineering structures, Volume 26.1, (2004), PP. 63-71.
8. Choi, Ji Hun, et al. "Experimental Evaluation of Internal Blast Resistance of Prestressed Concrete Tubular Structure according to Explosive Charge Weight." KSCE Journal of Civil and Environmental Engineering Research, Volume 39.3, (2019), PP. 369-380.
9. Syed Zubair Imam, Osama Ahmed Mohamed, and Shaikh Atikur Rahman. "Non-linear finite element analysis of offshore stainless steel blast wall under high impulsive pressure loads." Procedia Engineering, Volume 145, (2016), PP.1275-1282.
10. Manmohan Dass Goel, Vasant Matsagar, "Blast-Resistant Design of Structures." ASCE, Practice Periodical design on Structural Design and construction, May (2014).
11. Saleh E. Ibrahim, Mostafa A. Ismail, Marwa Nabil, "Response of Reinforced Concrete Frame Structures Under Blast Loading." Sustainable Civil Engineering Structures and Construction Materials, SCESCM (2016).
12. T. Ngo, P. Mendis, Luccioni, and Rodolfo Francisco Danesi. "Analysis of building collapse under blast loads.", Engineering structures, Volume 26.1, 2001, PP. 63-71.

